catalysts

MDPI

Article

Electrochemical Degradation of Nitrobenzene Wastewater: From Laboratory Experiments to Pilot-Scale Industrial Application

Dunyi Liu [1,*], Zhangjiu Liao [1], Ziyi Hu [1] and Enxiang Shang [2]

[1] College of Resources and Environment, Southwest University, Chongqing 400715, China; lzj7002020@email.swu.edu.cn (Z.L.); huziyi@email.swu.edu.cn (Z.H.)
[2] College of Science and Technology, Hebei Agricultural University, Huanghua 061100, China; shangenx@163.com
* Correspondence: liudy1989@swu.edu.cn

Abstract: In this study, the electrochemical degradation of nitrobenzene (NB) was conducted on the Ti/SnO_2-Sb/Ce-PbO_2 anode with excellent functional performance. The effect of applied current density, electrode distance, pH value and initial concentration on the reaction kinetics of NB was systematically studied. The total organic carbon (TOC) removal rate reached 91.5% after 60 min of electrolysis under optimal conditions. Eight aromatic intermediate products of NB were identified by using a gas chromatography coupled with a mass spectrometer, and two aliphatic carboxylic acids were qualitatively analyzed using a high-performance liquid chromatograph. The electrochemical mineralization mechanism of NB was proposed based on the detected intermediates and the identified key active oxygen specie. It was supposed that the hydroxyl radical produced on an anode attacked NB to form hydroxylated NB derivatives, followed by the benzene ring opening reactions with the formation of aliphatic carboxylic acids, which mineralized to CO_2 and H_2O. In addition, NB was reduced to less stable aniline on the cathode surface, which resulted in actualized mineralization. The successful pilot-scale industrial application in combination with wastewater containing NB with the influent concentration of 80–120 mg L^{-1} indicated that electrochemical oxidation has great potential to abate NB in practical wastewater treatment.

Keywords: nitrobenzene; electrochemical oxidation; mineralization; mechanisms; industrial application

Citation: Liu, D.; Liao, Z.; Hu, Z.; Shang, E. Electrochemical Degradation of Nitrobenzene Wastewater: From Laboratory Experiments to Pilot-Scale Industrial Application. *Catalysts* **2022**, *12*, 190. https://doi.org/10.3390/catal12020190

Academic Editor: Carlo Santoro

Received: 27 December 2021
Accepted: 31 January 2022
Published: 2 February 2022

1. Introduction

Nitrobenzene ($C_6H_5NO_2$, NB) is widely used as a raw material and an intermediate product for the manufacture of anilines, pesticides, pharmaceuticals, explosives and dyes [1,2]. NB cannot be efficiently removed by traditional activated sludge technology due to its strong electronegativity of the nitro-group which decreases the electron density of the benzene ring [3,4]. In addition, NB and its transformation metabolites have an inhibition effect on microbial activity in the biological treatment process due to toxicity and mutagenicity [5–7], which leading to the accumulation of NB in the environment. A previous study reported that it accounted for 80% of surface water contaminated by NB in China, with the residual concentration ranging from <0.3 ng L^{-1} to 8450.0 ng L^{-1} [8].

The ubiquity of NB has drawn increasing attention due to its potential hazard to aquatic systems and to human beings [9–11]. The 96 h sublethal concentration (LC_{50}) values of NB on *Daphnia pulex* and *Ciprinus carpio* were determined to be 0.760 mg L^{-1} and 1.907 mg L^{-1}, respectively [12]. The genotoxicity of NB, which could induce micronuclei in mammalian cells, has also been reported [13]. NB is listed as a priority pollutant [14] and is classified as a Group B2 carcinogen [15]. The permission concentration for NB in the

surface water is restricted to 17 μg L^{-1} in China for environmental security [16]. Therefore, it is crucial to seek a dependable way to eliminate NB from wastewater.

Advanced oxidation processes (AOPs) have recently been utilized for treatment of refractory organic pollutants, mainly due to their ability to produce highly oxidizing radicals, e.g., hydroxyl radical (•OH) [17,18]. It has been demonstrated that NB could be efficiently removed by ozonation [19–21], photocatalysis [22,23] and the Fenton reaction [18,24]. Nevertheless, strict operational conditions constrained the application of these AOPs, or the subsequent sludge disposal increased the invested cost of the wastewater treatment plants. Thus, it is still urgent to develop an efficient, feasible alternative approach to decompose NB in wastewater.

Electrochemical oxidation is considered an environmental-friendly technology for the purification of chemical industry wastewater [17]. The degradation efficiency of electrochemical oxidation primarily depends on the choice of anode materials on which the pollutants can be degraded by direct and indirect oxidation reactions [25,26]. Ce-doped PbO_2 electrodes with SnO_2-Sb as the middle layer (Ti/SnO_2-Sb/Ce-PbO_2) have been proven to possess high chemical stability and good performance on the removal of a variety of recalcitrant pollutants, e.g., perfluorocarboxylic acids [27,28], sulfamethoxazole [29], ibuprofen [26], and phenol [30] from aqueous solutions. However, it is yet to be determined whether NB can be degraded by the Ti/SnO_2-Sb/Ce-PbO_2 anode. Moreover, laboratory experiments applying the electrochemical oxidation process to decontaminate various wastewaters, including dye wastewater [31,32], pharmaceuticals and personal care products [33,34] and coking wastewater [35], have been extensively conducted and have effectively clarified its advantages, but very little information is available on the industrial application.

This paper presents the feasibility of the electrochemical oxidation process using Ti/SnO_2-Sb/Ce-PbO_2 anode for the treatment of NB wastewater on an industrial scale. To optimize the process parameters, electrolysis of NB was carried out under different applied current densities, electrode distances, solution pHs, and initial NB concentrations in the lab-scale experiment. The mineralization mechanism of NB was revealed based on identified intermediate organic byproducts, the trace of nitrogen atom, and the confirmed key active oxygen specie. Furthermore, a pilot-scale industrial electrochemical reaction system was developed and applied to clarify the potential practical application value for NB contaminated water.

2. Results and Discussion

2.1. Characterization of Anode

Figure 1a shows that the surface layer of the Ti/SnO_2-Sb/Ce–PbO_2 electrode is covered with dense polyhedron grains and that most of the grain sizes of particles are less than 1 μm. The nanostructure of the electrode can provide a striking number of reaction sites for the degradation of target pollutants. The lateral view SEM image of the prepared Ti/SnO_2-Sb/Ce-PbO_2 anodes is shown in Figure 1b. It was estimated that the average coating thickness of the anode was about 175 μm. Further energy dispersive spectrometer (EDS) element mapping (Figure 1c) revealed the uniform distribution of Pb, O and Ce, with the Ce/Pb stoichiometric ratios of about 0.1/23.3. Figure 1d shows that the characteristic peaks located at 2θ = 25.5, 32.1, 36.3, 49.2, 52.3, 59.0 and 62.6, correspond to the lattice planes (110), (101), (200), (211), (221), (310) and (301), respectively. The peak positions of the electrode corresponding to card number 73–0851 in the database are consistent with the tetragonal crystal structure of β-PbO_2. There are no obvious CeO_2 diffraction peaks in the XRD pattern, indicating a low doping level or that the rare earth element Ce is doped into the PbO_2 lattice.

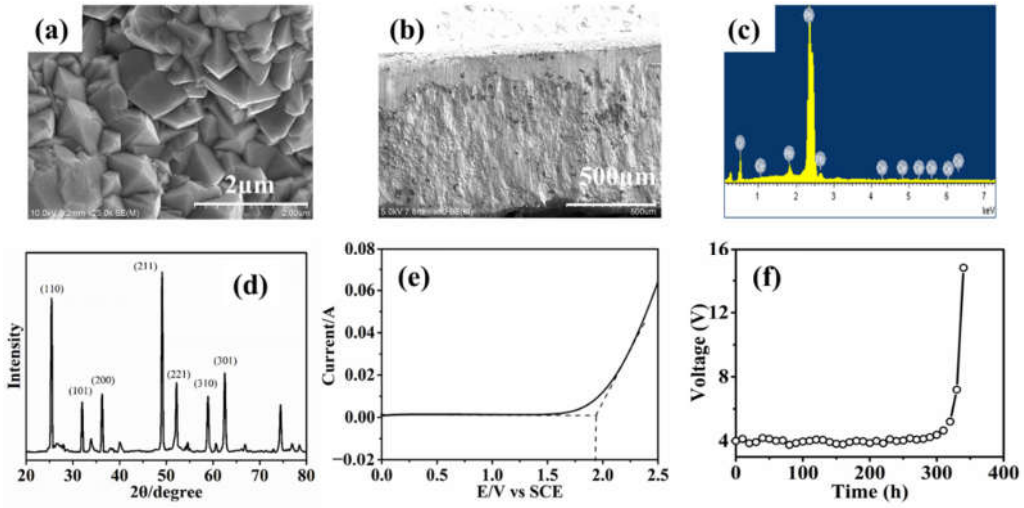

Figure 1. Top view (**a**) and lateral view (**b**); SEM images, EDS analysis (**c**); XRD pattern (**d**) of Ti/SnO_2-Sb/Ce-PbO_2 electrode; the linear sweep voltammetry of Ti/SnO_2-Sb/Ce-PbO_2 in 0.5 mol L^{-1} Na_2SO_4 solution at a scan rate of 100 mV s^{-1} (**e**); the variation trend of the cell potential over time in accelerated life test (H_2SO_4: 1 mol L^{-1}; current density: 1 A cm^{-2}) (**f**).

Figure 1c demonstrates that the oxygen evolution potential (OEP) of the prepared electrode is up to 1.92 V vs. SCE. Generally, the high OEP could effectively inhibit the oxygen evolution side-reaction which can enhance the degradation performance of the anode during an electrocatalytic degradation process. The mechanical and chemical stability is important in applications. The long-term electrochemical performance of Ti/SnO_2-Sb/Ce-PbO_2 anode was scrutinized by an accelerated life test conducted in extreme conditions (0.5 mol L^{-1} H_2SO_4 solution and high current density of 1 A cm^{-2}). As shown in Figure 1f, the accelerated service lifetime of the anode was 340 h. Obviously, the anode would have a much longer lifetime under mild conditions for wastewater treatment.

2.2. Electrochemical Degradation Kinetics of NB

In all laboratory experiments, the degradation of NB followed pseudo-first-order kinetics which can be described as follows:

$$-\frac{dc}{dt} = k_{NB}t$$

where k_{NB} and C are the pseudo-first-order rate constant (min^{-1}) and NB concentration (mg L^{-1}), respectively and t is the electrolysis time (min). Parameters including k_{NB}, half-lives ($t_{1/2}$) and average voltage and correlation coefficient (R^2) are summarized in Table 1. Figure 2 presents the removal efficiency of NB as a function of current density, electrode distance, solution pH and initial NB concentration during the electrochemical oxidation process.

Table 1. Kinetics for NB degradation by Ti/SnO_2-Sb/Ce-PbO_2 anode.

Parameters		Rate Constant (k, min^{-1})	Half-Life (min)	Time Range (min)	Average Voltage (V)	R^2
Current density (mA cm^{-2})	1	2.7×10^{-2}	25.7	60	3.4	0.9998
	2	3.3×10^{-2}	21.0	60	4.2	0.9999
	5	4.5×10^{-2}	15.4	60	5.2	0.9996
	10	5.9×10^{-2}	11.7	60	6.6	0.9997
	20	7.8×10^{-2}	8.9	60	8.5	0.9996
	30	8.7×10^{-2}	8.0	60	10.5	0.9986
Electrode distance (cm)	0.5	1.2×10^{-1}	5.8	40	5.0	0.9989
	1.0	9.5×10^{-2}	7.3	50	5.9	0.9993
	1.5	7.8×10^{-2}	8.8	60	8.3	0.9990
	2.0	6.1×10^{-2}	11.4	60	9.2	0.9991
	3. 0	5.2×10^{-2}	13.3	60	10.6	0.9985
Initial pH	2	6.6×10^{-2}	9.6	60	6.8	0.9996
	5	7.7×10^{-2}	9.8	60	7.9	0.9988
	7	7.8×10^{-2}	9.6	60	7.7	0.9986
	9	7.4×10^{-2}	8.9	60	7.8	0.9987
	12	5.9×10^{-2}	11.7	60	7.5	0.9998
Initial concentration (C_0, mg L^{-1})	5	9.2×10^{-2}	7.5	30	9.1	0.9887
	10	8.5×10^{-2}	8.3	40	8.8	0.9918
	20	8.2×10^{-2}	8.4	60	8.7	0.9962
	50	7.7×10^{-2}	9.0	60	8.4	0.9982
	100	7.7×10^{-2}	9.0	60	8.2	0.9996
	200	8.0×10^{-2}	8.7	60	8.0	0.9997

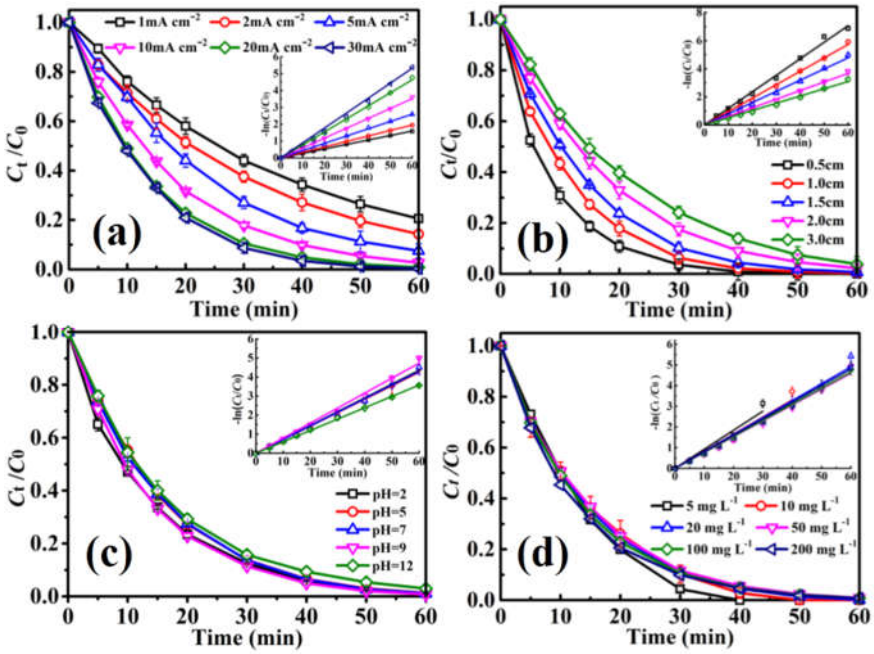

Figure 2. Effect of current density (**a**), electrode distance (**b**), solution pH (**c**), and initial NB concentration (**d**) on the degradation of NB. Insets are first-order kinetic model fit for NB degradation.

2.2.1. Effect of Applied Current Density

As shown in Figure 2a, increasing the applied current density can significantly enhance the NB removal rates. The k_{NB} values were measured to be 2.7×10^{-2}, 3.3×10^{-2}, 4.5×10^{-2}, 5.9×10^{-2}, 7.8×10^{-2} and 8.8×10^{-2} min^{-1} under the current density of 1, 2, 5, 10, 20 and 30 mA cm^{-2}, and the corresponding $t_{1/2}$ values were 25.7, 21.0, 15.4, 11.7, 8.9 and

8.0 min, respectively (see Table 1). It was apparent that the degradation efficiency of NB improves with increasing the current density. It was conjectured that a tremendous amount of •OH production in the reaction system under a high current density resulted in NB molecules being instantaneously degraded [36,37]. It was noted that the removal rate of NB was slightly increased 0.3% (from 99.4% to 99.7%) when the current density was increased from 20 mA cm^{-2} to 30 mA cm^{-2}, whereas the energy cost (calculated by Equation (S1) in Text S1 in Supplementary Materials) was greatly increased by 20% (from 86.3 ± 3 Wh L^{-1} to 103.5 ± 2 Wh L^{-1}). It could be conjectured that undesirable side reactions, such as water splitting reaction and oxygen evolution, were particularly pronounced as the current density increased; the observation of intensive bubbles on electrode surface verified this conjecture [38].

2.2.2. Effect of Electrode Distance and pH

The electrode distance affects the diffusion rate of the target pollutant in the electrochemical oxidation system, which has an impact on its degradation efficiency [38]. Figure 2b suggests that complete removal of NB can be achieved with an electrode distance of 0.5 cm and 1.0 cm with 50 min electrolysis. When the electrode distance is 2.0 cm or 3.0 cm, NB cannot be entirely removed after 60 min. Table 1 shows that the k_{NB} value decreased significantly with increased electrode distance, which can be explained by the fact that NB molecules can rapidly diffuse from bulk solution to anode surface at shorter electrode distance, and thus improve the electrochemical selectivity of •OH for NB [29]. Nevertheless, taking various factors, e.g., treatment efficiency, space efficiency, the short-circuit problem of the system and the investment costs, into consideration for the practical application, a relative larger electrode distance (i.e., 1.5 cm) is required.

The solution pH typically influences the degradation efficiency, and the pH fluctuation is commonly found for practical industrial wastewater [9]. Hence, the influence of the solution pH was investigated at a wide range (2.0–12.0) (Figure 2c). As shown in Table S1, there was little difference in the degradation kinetics of NB at the investigated initial pH values. A slight decrease was observed at the initial pH of 2.0 (k_{NB} = 6.4 × 10^{-2} min^{-1}) and 12.0 (k_{NB} = 5.6 × 10^{-2} min^{-1}). It was because the generation of •OH was inhibited both in strong acidic and alkaline environments, resulting in the decrease of NB removal efficiency [9]. This indicated that the degradation of NB on the Ti/SnO_2-Sb/Ce-PbO_2 anode can be performed at wide pH ranges, which will undoubtedly apply to NB wastewater.

2.2.3. Effect of Initial NB Concentration

The effect of the initial NB concentration, ranging from 5.0 mg L^{-1} to 200.0 mg $L^{-1,}$ was investigated, and the result is shown in Figure 2d. It is clearly that entire elimination of NB was accomplished within 60 min electrolysis for all test levels. Table 1 highlights that the degrade rate constant of NB was slightly decreased from 9.2 × 10^{-2} to 7.7 × 10^{-2} min^{-1} with the initial concentration increasing from 5 to 50 mg L^{-1}. This phenomenon was because the amount of •OH radicals produced in this reaction system were constant under certain current density [4], resulting in a higher probability that NB molecules would be oxidized by •OH at relative lower initial NB concentrations. At the same time, the k_{NB} values were similar for higher NB concentrations ranging from 50 to 200 mg L^{-1}. Despite a lower ratio of •OH to NB at higher initial concentrations, more NB molecules can react with the •OH radicals on the anode surface, leading to a fast degradation rate.

Considering the requirement of high removal efficiency of NB and low energy cost, the current density of 20 mA cm^{-2} was recommended in the pilot-scale industrial application. The electrode distance of 1.5 cm was adopted based on the treatment efficiency and practical problems which have been stated in Section 2.2.2. The solution pH has little effect on the degradation efficiency of NB, however, overly acidic and alkaline conditions cause corrosion of electrodes and other devices, resulting in increased operating costs. Therefore, the aqueous solution needs to be properly adjusted in practical applications if the pH of the wastewater is overly acidic or alkaline. The NB concentration in the influent of the

designed electrochemical reaction unit was about 80~120 mg L^{-1} within the investigated range, which made it possible for high performance of the electrochemical system using the Ti/SnO_2-Sb/Ce-PbO_2 anode.

2.3. The Mineralization of NB under the Optimum Conditions

2.3.1. Evolution of TOC and Nitrogen-Containing Final Products

Though some techniques could also largely remove NB from water, they may yield toxic byproducts, such as nitrosobenzene and aniline [5–7]. To examine the mineralization degree of NB in the optimized electrochemical oxidation system (i.e., current density of 20 mA cm^{-2}, the electrode distance of 1.0 cm, pH without adjustment, and the initial concentration of 100 mg L^{-1}), the TOC removal rate and the evolution of nitrogen-containing inorganic products were fully examined at optimized conditions. As is evident from Figure 3, the TOC removal rate achieved 91.5% after 60 min of electrolysis, which implies that most NB molecules and their intermediate byproducts were simultaneously oxidized by the electrochemical oxidation process. The mineralization process of heterocyclic compounds is typically accompanied by the formation of inorganic ions. Ammonium (NH_4^+), nitrate (NO_3^-), and nitrite (NO_2^-) ions were observed during the electrochemical oxidation of NB, and the concentration trends of NO_3^--N, NO_2^--N, NH_4^+-N and total nitrogen (TN) are shown in Figure 3. The denitration reaction of nitro groups resulted in the occurrence of NO_2^-, which was further converted to NO_3^- on the anode surface. The generation of NH_4^+ can be explained by consecutive reductive reactions of nitro group or the direct reduction process of the produced NO_2^- on the cathode surface. The concentration of NO_3^--N was accumulated to 6.2 mg L^{-1}; nevertheless, the concentrations of NO_2^--N and NH_4^+-N were much lower compared with those of NO_3^--N, which can be partially due to the instability of the NO_2^- and NH_4^+ ions. Notably, the mass balance of TN gradually decreased with electrolysis time, and the TN concentration was progressively reduced from 11.3 to 7.6 mg L^{-1}. We hypothesize that the fraction of the nitrogen atom left the solution in the form of N_2 and/or was adsorbed on electrode surface might be responsible for this phenomenon.

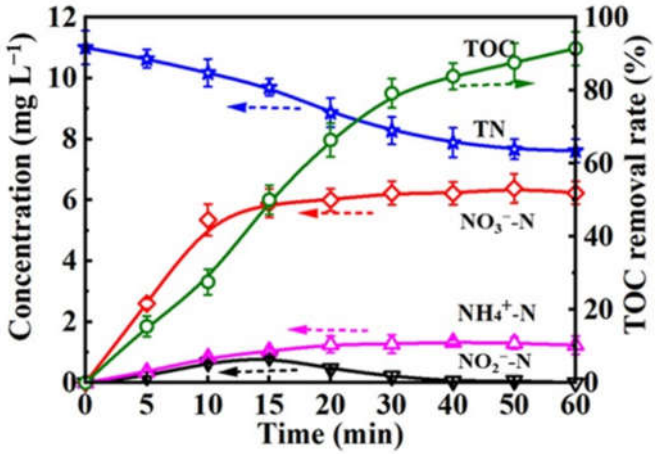

Figure 3. The evolution of NO_3^--N, NO_2^--N, NH_4^+-N and TN concentrations, and the corresponding TOC removal rates during the electrochemical oxidation of 100 mg L^{-1} NB (Current density of 20 mA cm^{-2}, electrode distance of 1.5 cm).

2.3.2. Qualitative and Quantitative Determination of •OH

Generally, •OH is considered as the key active oxygen specie in the electrochemical oxidation system. It was noted that Na_2SO_4 is routinely added to the solution as a supporting electrolyte to increase ionic conductivity. It is worth highlighting that when sulfates are used, the persulfates may be generated at non-active anodes [39]. In order to discern the key active oxygen free radical that causes the mineralization of NB, tertiary

butyl alcohol (TBA) and methanol (MeOH) were added into the system as scavengers, and the result is shown in Figure 4a. Apparently, the removal rate of NB was significantly decreased when adding 50 mM TBA/MeOH to the reaction electrolyte, with the k_{NB} decreased from 7.8×10^{-2} min^{-1} to 2.4×10^{-2} min^{-1} and 2.1×10^{-2} min^{-1}, respectively. Further increasing the scavenger concentration to 500 mM caused a notable decrease of reduction in NB oxidation kinetics (3.3×10^{-3} min^{-1} with 500 mM TBA, 2.8×10^{-3} min^{-1} with 500 mM MeOH). By comparing the reaction rate constant of scavengers and active oxygen species, TBA was generally observed as •OH scavenger and MeOH was observed as •OH and $SO_4^{\bullet -}$ scavenger [40–42]. The above analyses indicate that •OH was the main active oxygen specie during the electrochemical oxidation reaction. Of particular note, the removal rate of NB was still able to reach 15.4% despite the existence of 500 mM MeOH, which might be due to the effect of other active oxygen species, e.g., $O_2^{\bullet -}$, or the direct oxidation of NB on the anode. On the other hand, the active oxygen species would not be completely quenched by the scavenger, leading to small degradation of NB.

Salicylic acid was utilized as a probe to quantify the concentration of •OH generated in this electrochemical oxidation system with an applied current density of 20 mA cm^{-2} (detailed see Text S2). As shown in Figure 4b, the generation of •OH in this process followed typical pseudo-first-order kinetics, and the theoretical production rate constant of •OH was calculated to be 47.1 mM min^{-1} m^{-2}. •OH was a non-specific oxidant, which could react with most organic pollutants [43]. The aforementioned results suggest that •OH was the main active specie, and the high production could ensure the high mineralization rate of NB.

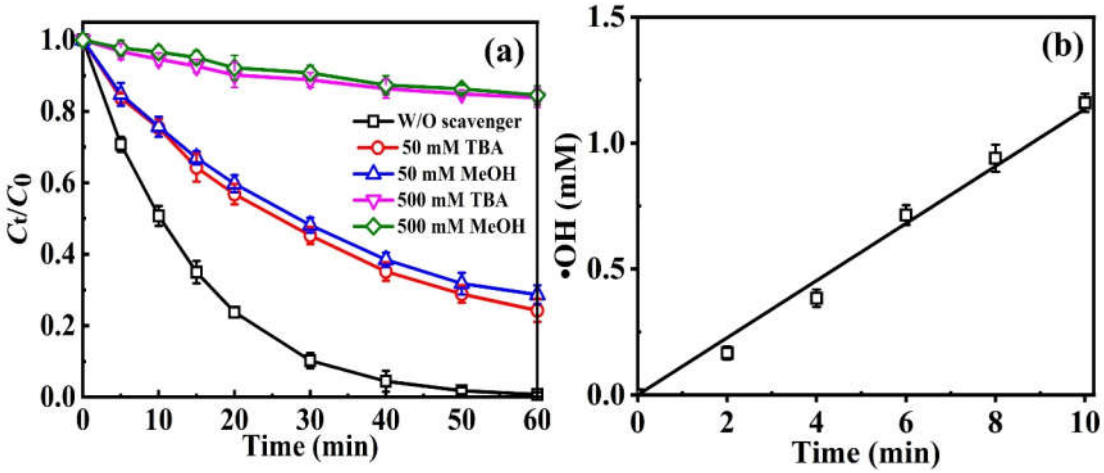

Figure 4. The effect of scavengers on the degradation of NB (**a**) and production of •OH (**b**) during electrochemical system. (Current density of 20 mA cm^{-2}, plate distance of 1.5 cm, NB of 100 mg L^{-1}).

2.3.3. Intermediate Analysis and Degradation Pathway

Some intermediate byproducts, e.g., nitrophenols, aniline and organic acids, which have adverse effects on environmental health and human beings, are normally detected during the degradation of NB by AOPs [44–46]. To better elucidate the mineralization mechanism of NB by electrochemical oxidation on the fabricated anode, the intermediates were recognized with the assistance of a gas chromatograph coupled with a mass spectrometer (GC-MS) and a high-performance liquid chromatograph (HPLC). Eight aromatic intermediates of NB were detected based upon the MS fragmentation pattern, "nitrogen rule" and relevant literatures. Detailed information of the detected intermediates is shown in Table S1. The transformations of the intermediate structures included the denitration and substitution of nitro group by hydroxyl group (phenol), the formation of a ketone group on the benzene ring (benzoquinone) and the hydroxylation of the benzene ring (*o*-Nitrophenol, *m*-Nitrophenol and *p*-Nitrophenol). Meanwhile, two isomers, resorcinol and hydroquinone were also detected. The entities of the above intermediates are commonly

reported byproducts by other oxidation processes, e.g., anodic oxidation [17], Fenton-like catalytic degradation with Fe-Cu bimetallic catalysts [3], and photodegradation with ZnO_2 nanoparticles [47]. It was noted that aniline was quantified by GC-MS, which implies that the reduction reaction of NB also exists in this degradation system. Moreover, two aliphatic carboxylic acid intermediates, including maleic acid and oxalic acid, were identified by HPLC, indicating that aromatic intermediates were further decomposed into low molecular-weight carboxylic acids.

Based on the identified intermediates and the qualitative key reactive specie (•OH), the possible degradation pathway of NB was proposed (see Figure 5). The α-, β- and γ-carbons of the aromatic ring of NB were attacked by •OH, accompanied by the formation of three nitrophenol isomers (*o*-Nitrophenol, *m*-Nitrophenol and *p*-Nitrophenol). Subsequently, the nitro group of nitrophenol was further attacked by •OH, resulting in denitration and the formation of dinitrophenols. The released NO_2^- ion might have simultaneously oxidized or reduced on the anode or cathode. The presence of NO_3^- and NH_4^+ could indirectly verify this hypothesis. On the other hand, the nitro group of NB with strong electron-withdrawing characteristics could be electrophilic and attacked by •OH to form phenol. It is noteworthy that the reduction of NB also occurred on the cathode leading to the formation of aniline, which was also identified in other synchronistic oxidation and reduction systems [9,48]. Then, the substitution of $–NH_2$ by the –OH group could generate the product phenol with the release of NH_4^+. The further oxidation of phenol by •OH led to the formation of dinitrophenols. Then, hydroquinone was dehydrogenated to benzoquinone. In the subsequent stage, the aromatic intermediates underwent a series of oxidation reactions by •OH attack, resulting in the ring cleavage to form aliphatic carboxylic acids, including maleic and oxalic acids. These small molecule acids were finally oxidized into CO_2 and H_2O, which was verified by the high mineralization rate of NB.

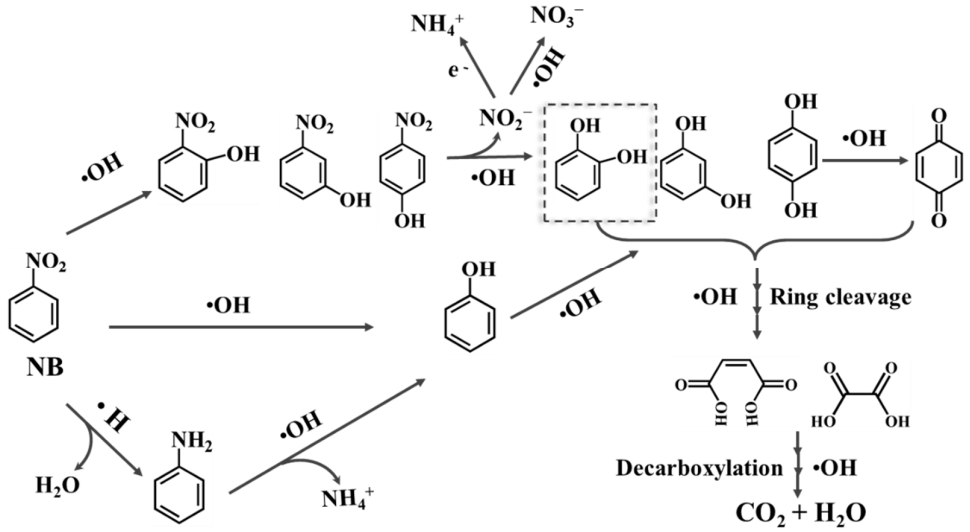

Figure 5. Proposed mineralization pathways of NB by electrochemical degradation.

2.4. Pilot-Scale Industrial Application

To explore the feasibility of electrochemical oxidation using Ti/SnO_2-Sb/Ce-PbO_2 anode in industrial applications, a pilot-scale application was investigated in one chemical plant which is described in greater detail in Section 3.2. The static degradation experiment was conducted under optimized laboratory conditions, i.e., applied current density of 20 mA cm^{-2} and electrode distance of 1.5 cm. Figure 6 shows that the degradation rate of NB and COD in the wastewater were 96.2% and 68.8%, respectively. Obviously, compared to a laboratory experiment, a real NB wastewater experiment involves difficult challenges. However, it could improve the biodegradability subsequent biological treatment. Signifi-

cantly, there was no significant change for the COD removal after 90 min of electrolysis, so the hydraulic retention time was kept at 90 min in the sequential treatment.

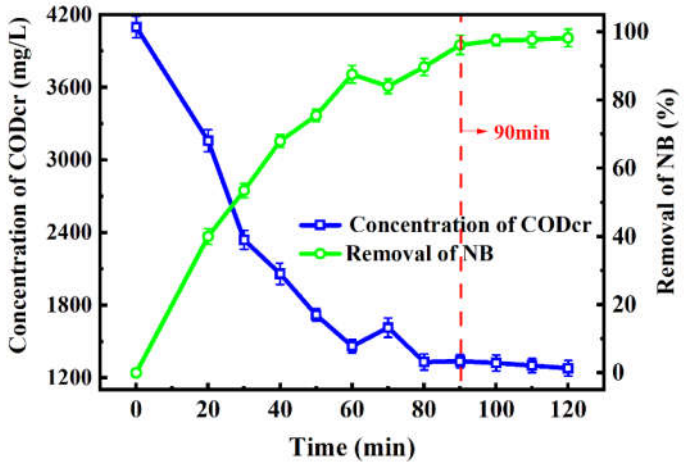

Figure 6. The static degradation experiment in a pilot-scale electrochemical reaction system. Applied current density: 20 mA cm^{-2}; electrode distance: 15 mm; volume of wastewater: 827.5 L.

Although existing processes of Fenton oxidation and flocculant precipitant can remove most organic pollutants and meet the quality requirement of the influent into a biological unit, their disadvantages, such as unstable water quality, extra additives of Fenton's reagent and flocculant, and large amounts of chemical sludge, are many. Hoping to resolve the above-mentioned problems, the electrochemical oxidation equipment was installed to replace original Fenton and flocculant units. As shown in Figure 7, the concentration of NB in the effluent was 2.14–4.73 mg L^{-1} and the COD was 1106–1520 mg L^{-1} at the average inlet flow of 0.55 m^3 h^{-1} within a 30 d pilot run time. Obviously, the effectiveness of electrochemical oxidation was superior to the replaced Fenton-flocculation process. In addition, Table S2 gives a rough estimate of the economic costs of the electrochemical oxidation unit and the replaced Fenton-flocculant precipitant process. Results show that the operating cost for the electrochemical oxidation unit accounted for only 18.8% of the cost of the replaced Fenton-flocculant precipitant process, showing the economic feasibility of the application of electrochemical oxidation in this chemical plant.

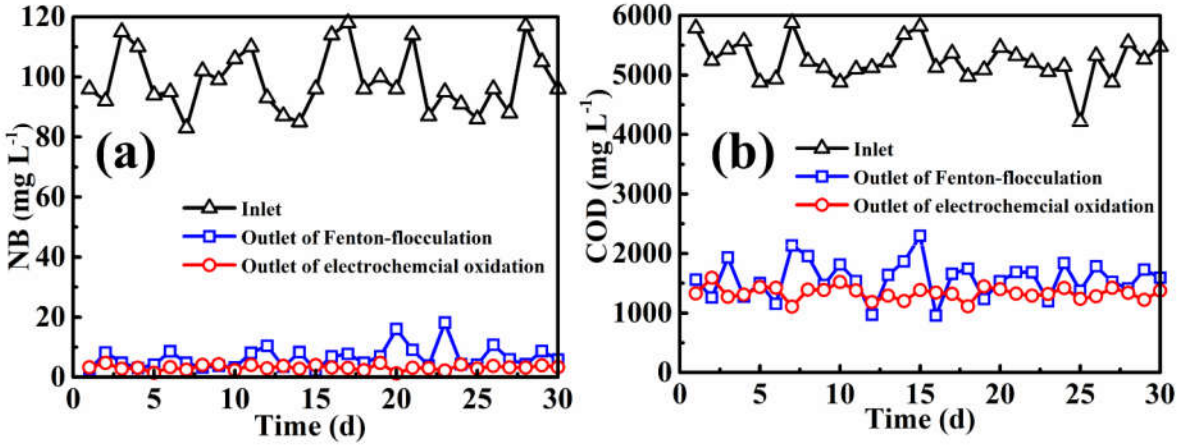

Figure 7. The concentration of NB (**a**) and COD (**b**) before and after treatment in the pilot-scale electrochemical reaction system with the average flow of 0.55 m^3 h^{-1}. Applied current density: 20 mA cm^{-2}; electrode distance: 15 mm; volume of wastewater: 827.5 L; hydraulic retention time of 90 min.

3. Materials and Methods

3.1. Laboratory Experiments

The preparation process of the Ti/SnO_2-Sb/Ce-PbO_2 electrode was identical to the previous study [26]. Briefly, titanium sheets were sanded with 200, 600 and 800 grit sandpaper, and then immersed in 10% NaOH solution and etched with a 5% boiling oxalic acid solution. Subsequently, the middle layer (SnO_2-Sb) was prepared by the sol-gel technique with the coating solution (the molar ratio of ethylene glycol, citric acid, $SnCl_4 \cdot 4H_2O$ and $SbCl_3$ was 140:30:9:1). The Ce-PbO_2 layer was acquired by electrodeposition with Ti/SnO_2-Sb as the anode. The electrodeposition was conducted under 20 mA cm^{-2} for 60 min, and the electrolyte consisted of 0.1 M HNO_3, 200 g L^{-1} $Pb(NO_3)_2$, 0.4 g L^{-1} $Ce(NO_3)_3$ and 0.5 g L^{-1} NaF. The relevant preparation details are provided in Text S3. In the lab-scale electrochemical experiments, the prepared electrode (50 mm × 50 mm × 1 mm) served as the anode, and a titanium sheet (purity 99.9%) with the same dimensions was used as the cathode. The surface morphology of the anode was investigated using scanning electron microscopy (SEM/EDS, S4800, Hitachi, JPN). The crystal phase composition and crystallinity of the anode were examined with X-ray diffraction (XRD) (PANalytical, Almelo, NL). The electrochemical measure was conducted in a conventional three-electrode cell system on a CHI660E electrochemical workstation (CH Instruments, Shanghai, CHN). The prepared anode, a platinum plate, and a saturated calomel electrode (SCE) were used as the working, counter, and reference electrodes, respectively. The linear sweep voltammetry (LSV) test was conducted in 0.5 mol L^{-1} Na_2SO_4 solution with a scan rate of 50 mV s^{-1}. The accelerated service lifetime tests were performed at the current density of 1 A cm^{-2} in the 0.5 mol L^{-1} H_2SO_4 solution. Inactivation of electrode occurred when the recorded cell voltage was 5 V higher than the initial value.

The effect of applied current density (1–30 mA cm^{-2}) and initial pH values (2.0–12.0) were investigated in a 30 mL reaction solution with initial NB concentration of 100 mg L^{-1}. To examine the effect of electrode distances (0.5–3.0 cm), 30–100 mL of 100 mg L^{-1} NB solution was used to conduct the experiment. Furthermore, the effect of initial NB concentrations (5.0–200.0 mg L^{-1}) was investigated to effectively evaluate the application scope of the electrochemical oxidation. To increase the conductivity, 35 mM Na_2SO_4 was added in all solutions as a supporting electrolyte.

3.2. Pilot-Scale Industrial Application

The chemical plant is located in Huaian, Jiangsu province in China, and its main commercial products are dinitrotoluene and toluidine. The load of industrial wastewater is about 30 m^3 h^{-1}, and the dominant organic pollutant is NB. Original wastewater treatment processes mainly included Fenton oxidation, flocculant precipitant, bio-contact oxidation and ozone discoloring. The influent concentrations of NB and COD are 80–120 mg L^{-1} and 4000~6000 mg L^{-1}, respectively, for the Fenton oxidation unit. The scheme of the pilot-scale electrochemical reaction system is shown in Figure 8. The electrolytic cells were made of polymethyl methacrylate undivided with the dimensions of 1.5 m × 0.8 m × 0.8 m. The electrodes were connected in the series mode. The Ti/SnO_2-Sb/Ce-PbO_2 anode (50 cm × 50 cm × 0.1 cm) and titanium sheet with the same size were fixed on the reactor. The top of the reactor set up A skimming dish was set up on the top of the reactor; and a dustpan shaped sludge collecting hopper was set up on the bottom. The wastewater was pumped from the bottom, with an outlet on the top of the reactor. Other operation parameters were designed on the basis of the results of laboratory experiments. The flowcharts of the wastewater treatment units before and after the application are represented in Figure S1. The requirement of the chemical plant was that the concentrations of NB and COD be lower than 5 mg L^{-1} and 1500 mg L^{-1} in the effluent of the electrochemical oxidation unit.

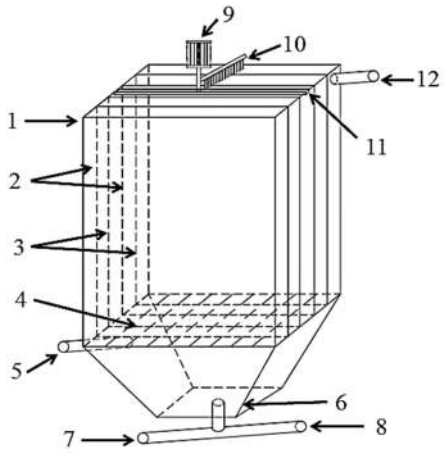

Figure 8. The scheme of the pilot-scale industrial electrochemical reaction system: 1—the shell of the reaction; 2—anodes; 3—cathodes; 4—grille; 5—inlet pipe; 6—dustpan shaped collecting hopper; 7—wash water pumps; 8—deslagging pipe; 9—DC power supply; 10—skimming dish; 11—fixed link; 12—outlet pipe.

3.3. Analytical Methods

The concentrations of NB were measured using HPLC Dionex U3000 (Thermo Fisher, Waltham, MA, USA) with a dual absorbance detector (DAD). The separation was performed on an Athena C18-WP (4.6 mm × 250 mm, 5 μm particle size) column. The mobile phase was ultrapure water and methanol (30/70, v/v). The detected ultraviolet absorption wavelength was 265 nm. and the flow velocity was set at 1 mL min^{-1} with an injection volume of 20 μL.

Intermediate products of NB formed in the reaction system were characterized by GC-MS (7890A-5975C, Agilent, Santa Clara, CA, USA) equipped with a DB-5MS column (30 m × 0.25 mm, 0.25 μm particle size). The initial GC column was kept at 50 °C for 2 min, then increased to 300 °C with a rate of 20 °C min^{-1}. Notably, each individual sample was extracted dichloromethane three times before the GC-MS analysis. In addition, qualitative determination of the generated carboxylic acids was performed by HPLC-UV, using a HSS XSelect T3-C18 column (2.1 mm × 100 mm, 2.5 μm particle size). The ultraviolet absorption wavelength was 220 nm, and the mobile phase was 4 mmol L^{-1} H_2SO_4 with a flow velocity of 0.4 mL min^{-1}.

The TOC and TN of the electrolyte were measured on a TOC-L-CPH/CPN analyzer (Shimadzu, Kyoto, Japan). Concentrations of ammonia nitrogen (NH_4^+-N) were measured using HJ 535-2009 Water Quality Determination of Ammonia Nitrogen-Nessler's Reagent Spectrophotometry. The concentrations of nitrate ion (NO_3^-) and nitrite ion (NO_2^-) in the electrolyte were detected using an ion chromatography system Dionex ICS-1000 (Thermo Fisher, Waltham, MA, USA).

4. Conclusions

NB can be effectively degraded and mineralized by electrochemical oxidation using a Ti/SnO_2-Sb/Ce-PbO_2 anode. The electrochemical degradation of NB followed pseudo-first-order kinetics and the k_{NB} increase with increasing current density and decreasing electrode distance. The solution pH and initial concentration of NB exhibited less impact on the removal of NB. Eight aromatic intermediates and two aliphatic carboxylic acid byproducts of NB were quantified using GC-MS and HPLC, respectively. A plausible electrochemical mineralization pathway of NB was proposed based on the identified intermediates, the qualitative and quantitative determination of the key active oxygen specie. The pilot-scale industrial experiment indicated that the concentration of NB and COD decrease to 2.14–4.73 mg L^{-1} and 1106–1520 mg L^{-1}, respectively, which effectively improves the biodegradability of wastewater and the stability of the effluent. Our findings

highlight the potential of a Ti/SnO_2-Sb/Ce-PbO_2 electrode for remediation of NB wastewater and provide support information for further industrial application of electrochemical oxidation technology.

Supplementary Materials: The following are available online at https://www.mdpi.com/article/10.3390/catal12020190/s1, Text: S1, Text: S2, Text: S3, Figure S1: The flowcharts of the wastewater treatment processes before (a) and after (b) reform in the chemical plant; Table S1: Intermediates of NB identified by GC-MS/MS in electrospray ionization positive mode, Table S2: The operating costs of electrochemical oxidation unit and the replaced Fenton-flocculant precipitant process.

Author Contributions: Conceptualization, D.L. and E.S.; methodology, D.L. and Z.L.; formal analysis, D.L. and Z.H.; resources, D.L.; writing—original draft preparation, D.L.; writing—review and editing, D.L. and E.S.; supervision, D.L.; funding acquisition, D.L. and E.S. All authors have read and agreed to the published version of the manuscript.

Funding: This research was funded by the Natural Science Foundation of Hebei Province (No. B2019204315) and the Fundamental Research Funds for the Central Universities (XDJK2019C063).

Data Availability Statement: Not applicable.

Acknowledgments: We are grateful for the technical support by Chong Wang in Southwest University.

Conflicts of Interest: The authors declare no conflict of interest. The funders had no role in the design of the study; in the collection, analyses, or interpretation of data; in the writing of the manuscript or in the decision to publish the results.

References

1. Lv, T.; Wu, S.; Hong, H.; Chen, L.; Dong, R. Dynamics of nitrobenzene degradation and interactions with nitrogen transformations in laboratory-scale constructed wetlands. *Bioresour. Technol.* **2013**, *133*, 529–536. [CrossRef] [PubMed]
2. Cai, Z.; Fu, J.; Du, P.; Zhao, X.; Hao, X.; Liu, W.; Zhao, D. Reduction of nitrobenzene in aqueous and soil phases using carboxymethyl cellulose stabilized zero-valent iron nanoparticles. *Chem. Eng. J.* **2018**, *332*, 227–236. [CrossRef]
3. Sun, Y.; Yang, Z.; Tian, P.; Sheng, Y.; Xu, J.; Han, Y. Oxidative degradation of nitrobenzene by a Fenton-like reaction with Fe-Cu bimetallic catalysts. *Appl. Catal. B Environ.* **2019**, *244*, 1–10. [CrossRef]
4. Zhao, J.; Zhu, C.; Lu, J.; Hu, C.; Peng, S.; Chen, T. Electro-catalytic degradation of bisphenol A with modified Co3O4/β-PbO2/Ti electrode. *Electrochim. Acta* **2014**, *118*, 169–175. [CrossRef]
5. Hao, X.; Zhou, M.; Xin, Q.; Lei, L. Pulsed discharge plasma induced Fenton-like reactions for the enhancement of the degradation of 4-chlorophenol in water. *Chemosphere* **2007**, *66*, 2185–2192. [CrossRef] [PubMed]
6. Liu, G.; Dong, B.; Zhou, J.; Wang, J.; Jin, R.; Li, J. Enhanced bioreduction of nitrobenzene by reduced graphene oxide materials: Effects of surface modification and coexisting soluble electron shuttles. *Environ. Sci. Pollut. Res.* **2017**, *24*, 26874–26880. [CrossRef] [PubMed]
7. Ji, Q.; Li, J.; Xiong, Z.; Lai, B. Enhanced reactivity of microscale Fe/Cu bimetallic particles (mFe/Cu) with persulfate (PS) for p-nitrophenol (PNP) removal in aqueous solution. *Chemosphere* **2017**, *172*, 10–20. [CrossRef]
8. Gao, J.; Liu, L.; Liu, X.; Zhou, H.; Wang, Z.; Huang, S. Concentration level and geographical distribution of nitrobenzene in Chinese surface waters. *J. Environ. Sci.* **2008**, *20*, 803–805. [CrossRef]
9. Han, Y.; Qi, M.; Zhang, L.; Sang, Y.; Liu, M.; Zhao, T.; Niu, J.; Zhang, S. Degradation of nitrobenzene by synchronistic oxidation and reduction in an internal circulation microelectrolysis reactor. *J. Hazard. Mater.* **2019**, *365*, 448–456. [CrossRef] [PubMed]
10. Jo, W.; Won, Y.; Hwang, I.; Tayade, R.J. Enhanced photocatalytic degradation of aqueous nitrobenzene using graphitic carbon–TiO2 composites. *Ind. Eng. Chem. Res.* **2014**, *53*, 3455–3461. [CrossRef]
11. Roy, P.; Periasamy, A.P.; Liang, C.; Chang, H. Synthesis of graphene-ZnO-Au nanocomposites for efficient photocatalytic reduction of nitrobenzene. *Environ. Sci. Technol.* **2013**, *47*, 6688–6695. [CrossRef]
12. Yen, J.; Lin, K.; Wang, Y. Acute lethal toxicity of environmental pollutants to aquatic organisms. *Ecotoxol. Environ. Saf.* **2002**, *52*, 113–116. [CrossRef] [PubMed]
13. Bonacker, D.; Stoiber, T.; Böhm, K.J.; Unger, E.; Degen, G.H.; Thier, R.; Bolt, H.M. Chromosomal genotoxicity of nitrobenzene and benzonitrile. *Arch. Toxicol.* **2004**, *78*, 49–57. [PubMed]
14. U.S. Environmental Protection Agency. *Ambient Water Quality Criteria for Nitrobenzene*; U.S. Environmental Protection Agency: Washington, DC, USA, 1980; Volume 10.
15. U.S. Environmental Protection Agency. *Guidelines for Carcinogen Risk Assessment—Federal Register*; U.S. Environmental Protection Agency: Washington, DC, USA, 2005; Volume 804, pp. 636–640.
16. State Environmental Protection Administration. *Environmental Quality Standard for Surface Water*; Regulation GHZB1-1999; State Environmental Protection Administration: Beijing, China, 1999.

17. Chen, Y.; Li, H.; Liu, W.; Tu, Y.; Zhang, Y.; Han, W.; Wang, L. Electrochemical degradation of nitrobenzene by anodic oxidation on the constructed TiO2-NTs/SnO2-Sb/PbO2 electrode. *Chemosphere* **2014**, *113*, 48–55. [CrossRef]
18. Zhang, Y.; Zhang, K.; Dai, C.; Zhou, X.; Si, H. An enhanced Fenton reaction catalyzed by natural heterogeneous pyrite for nitrobenzene degradation in an aqueous solution. *Chem. Eng. J.* **2014**, *244*, 438–445. [CrossRef]
19. Chen, C.; Yan, X.; Yoza, B.A.; Zhou, T.; Li, Y.; Zhan, Y.; Wang, Q.; Li, Q.X. Efficiencies and mechanisms of ZSM5 zeolites loaded with cerium, iron, or manganese oxides for catalytic ozonation of nitrobenzene in water. *Sci. Total Environ.* **2018**, *612*, 1424–1432. [CrossRef] [PubMed]
20. Ma, J.; Sui, M.; Zhang, T.; Guan, C. Effect of pH on MnOx/GAC catalyzed ozonation for degradation of nitrobenzene. *Water Res.* **2005**, *39*, 779–786. [CrossRef]
21. Zhao, L.; Sun, Z.; Ma, J. Novel relationship between hydroxyl radical initiation and surface group of ceramic honeycomb supported metals for the catalytic ozonation of nitrobenzene in aqueous solution. *Environ. Sci. Technol.* **2009**, *43*, 4157–4163. [CrossRef]
22. Nitoi, I.; Oancea, P.; Raileanu, M.; Crisan, M.; Constantin, L.; Cristea, I. UV–VIS photocatalytic degradation of nitrobenzene from water using heavy metal doped titania. *J. Ind. Eng. Chem.* **2015**, *21*, 677–682. [CrossRef]
23. Shen, X.; Zhu, L.; Wang, N.; Zhang, T.; Tang, H. Selective photocatalytic degradation of nitrobenzene facilitated by molecular imprinting with a transition state analog. *Catal. Today* **2014**, *225*, 164–170. [CrossRef]
24. ElShafei, G.M.; Yehia, F.Z.; Dimitry, O.; Badawi, A.M.; Eshaq, G. Degradation of nitrobenzene at near neutral pH using Fe^{2+}–glutamate complex as a homogeneous Fenton catalyst. *Appl. Catal. B Environ.* **2010**, *99*, 242–247. [CrossRef]
25. Sopaj, F.; Rodrigo, M.A.; Oturan, N.; Podvorica, F.I.; Pinson, J.; Oturan, M.A. Influence of the anode materials on the electrochemical oxidation efficiency. Application to oxidative degradation of the pharmaceutical amoxicillin. *Chem. Eng. J.* **2015**, *262*, 286–294. [CrossRef]
26. Wang, C.; Yu, Y.; Yin, L.; Niu, J.; Hou, L. Insights of ibuprofen electro-oxidation on metal-oxide-coated Ti anodes: Kinetics, energy consumption and reaction mechanisms. *Chemosphere* **2016**, *163*, 584–591. [CrossRef] [PubMed]
27. Lin, H.; Niu, J.; Xu, J.; Huang, H.; Li, D.; Yue, Z.; Feng, C. Highly efficient and mild electrochemical mineralization of long-chain perfluorocarboxylic acids (C9–C10) by Ti/SnO_2–Sb–Ce, Ti/SnO_2–Sb/Ce–PbO_2, and Ti/BDD electrodes. *Environ. Sci. Technol.* **2013**, *47*, 13039–13046. [CrossRef]
28. Niu, J.; Lin, H.; Xu, J.; Wu, H.; Li, Y. Electrochemical mineralization of perfluorocarboxylic acids (PFCAs) by Ce-doped modified porous nanocrystalline PbO_2 film electrode. *Environ. Sci. Technol.* **2012**, *46*, 10191–10198. [CrossRef] [PubMed]
29. Lin, H.; Niu, J.; Xu, J.; Li, Y.; Pan, Y. Electrochemical mineralization of sulfamethoxazole by Ti/SnO2-Sb/Ce-PbO2 anode: Kinetics, reaction pathways, and energy cost evolution. *Electrochim. Acta.* **2013**, *97*, 167–174. [CrossRef]
30. Xu, P.; He, X.; Mao, J.; Tang, Y. Fabrication of Ti/SnO_2 -Sb/Ce-PbO_2 anode from methanesulfonate bath and its electrocatalytic activity. *J. Electrochem. Soc.* **2019**, *166*, D638–D644. [CrossRef]
31. Katsaounis, A.; Souentie, S. Organic pollutants in water using DSA electrodes, in-cell mediated (via active chlorine) electrochemical oxidation. In *Encyclopedia of Applied Electrochemistry*; Springer: New York, NY, USA, 2014; pp. 1407–1416.
32. Panizza, M.; Cerisola, G. Electrocatalytic materials for the electrochemical oxidation of synthetic dyes. *Appl. Catal. B Environ.* **2007**, *75*, 95–101. [CrossRef]
33. Kitazono, Y.; Ihara, I.; Yoshida, G.; Toyoda, K.; Umetsu, K. Selective degradation of tetracycline antibiotics present in raw milk by electrochemical method. *J. Hazard. Mater.* **2012**, *243*, 112–116. [CrossRef]
34. Xu, L.; Niu, J.; Xie, H.; Ma, X.; Zhu, Y.; Crittenden, J. Effective degradation of aqueous carbamazepine on a novel blue-colored TiO2 nanotube arrays membrane filter anode. *J. Hazard. Mater.* **2021**, *402*, 123530. [CrossRef]
35. Wang, Y.; Sun, S.; Ding, G.; Wang, H. Electrochemical degradation characteristics of refractory organic pollutants in coking wastewater on multiwall carbon nanotube-modified electrode. *J. Nanomater.* **2012**, *2012*, 614032. [CrossRef]
36. Wang, C.; Niu, J.; Yin, L.; Huang, J.; Hou, L.A. Electrochemical degradation of fluoxetine on nanotube array intercalated anode with enhanced electronic transport and hydroxyl radical production. *Chem. Eng. J.* **2018**, *346*, 662–671. [CrossRef]
37. Wang, Y.; Shen, Z.; Chen, X. Effects of experimental parameters on 2,4-dichlorphenol degradation over Er-chitosan-PbO2 electrode. *J. Hazard. Mater.* **2010**, *178*, 867–874. [CrossRef] [PubMed]
38. Dai, Q.; Xia, Y.; Sun, C.; Weng, M.; Chen, J.; Wang, J.; Chen, J. Electrochemical degradation of levodopa with modified PbO2 electrode: Parameter optimization and degradation mechanism. *Chem. Eng. J.* **2014**, *245*, 359–366. [CrossRef]
39. Martínez-Huitle, C.A.; Rodrigo, M.A.; Sires, I.; Scialdone, O. Single and coupled electrochemical processes and reactors for the abatement of organic water pollutants: A critical review. *Chem. Rev.* **2015**, *115*, 13362–13407. [CrossRef]
40. Buxton, G.V.; Greenstock, C.L.; Helman, W.P.; Ross, A.B. Critical review of rate constants for reactions of hydrated electrons, hydrogen atoms and hydroxyl radicals (•OH/•O^-) in aqueous solution. *J. Phys. Chem. Ref. Data.* **1988**, *17*, 513–886. [CrossRef]
41. Clifton, C.L.; Huie, R.E. Rate constants for hydrogen abstraction reactions of the sulfate radical, SO_4^-. *Alcohols. Int. J. Chem. Kinet.* **1989**, *21*, 677–687. [CrossRef]
42. Neta, P.; Madhavan, V.; Zemel, H.; Fessenden, R.W. Rate constants and mechanism of reaction of sulfate radical anion with aromatic compounds. *J. Am. Chem. Soc.* **1977**, *99*, 163–164. [CrossRef]
43. Kavitha, V.; Palanivelu, K. Degradation of nitrophenols by Fenton and photo-Fenton processes. *J. Photochem. Photobiol. A Chem.* **2005**, *170*, 83–95. [CrossRef]

44. Zhang, L.; Shu, H.; Jia, Y.; Xu, D. Study on solid waste pyrolysis coke catalyst for catalytic cracking of coal tar. *Int. J. Hydrog. Energ.* **2020**, *45*, 19280–19290.
45. Lei, Z.; Gao, H.; Chang, X.; Zhang, L.; Wang, Y. An application of green surfactant synergistically metal supported cordierite catalyst in denitration of selective catalytic oxidation. *J. Clean. Prod.* **2019**, *249*, 119307. [CrossRef]
46. Wang, H.; Wang, J.; Bo, G.; Wu, S.; Luo, L. Degradation of pollutants in polluted river water using Ti/IrO_2-Ta_2O_5 coating electrode and evaluation of electrode characteristics. *J. Clean. Prod.* **2020**, *273*, 123019. [CrossRef]
47. Ramírez, J.I.D.L.; Villegas, V.A.R.; Sicairos, S.P.; Guevara, E.H.; Brito Perea, M.D.C.; Sánchez, B.L. Synthesis and characterization of zinc peroxide nanoparticles for the photodegradation of nitrobenzene assisted by UV-light. *Catalysts* **2020**, *10*, 1041. [CrossRef]
48. Qin, C.; Zhang, J.; Zhang, C.; He, Y.; Tratnyek, P.G. Abiotic transformation of nitrobenzene by zero valent iron under aerobic conditions: Relative contributions of reduction and oxidation in the presence of ethylene diamine tetraacetic acid. *Environ. Sci. Technol.* **2021**, *55*, 6828–6837. [CrossRef] [PubMed]